



This is a repository copy of *Effect of the activator dose on the compressive strength and accelerated carbonation resistance of alkali silicate-activated slag/metakaolin blended materials*.

White Rose Research Online URL for this paper:
<http://eprints.whiterose.ac.uk/90603/>

Version: Accepted Version

Article:

Bernal, S.A. (2015) Effect of the activator dose on the compressive strength and accelerated carbonation resistance of alkali silicate-activated slag/metakaolin blended materials. *Construction and Building Materials*, 98. 217 -226. ISSN 0950-0618

<https://doi.org/10.1016/j.conbuildmat.2015.08.013>

Article available under the terms of the CC-BY-NC-ND licence
(<https://creativecommons.org/licenses/by-nc-nd/4.0/>)

Reuse

Unless indicated otherwise, fulltext items are protected by copyright with all rights reserved. The copyright exception in section 29 of the Copyright, Designs and Patents Act 1988 allows the making of a single copy solely for the purpose of non-commercial research or private study within the limits of fair dealing. The publisher or other rights-holder may allow further reproduction and re-use of this version - refer to the White Rose Research Online record for this item. Where records identify the publisher as the copyright holder, users can verify any specific terms of use on the publisher's website.

Takedown

If you consider content in White Rose Research Online to be in breach of UK law, please notify us by emailing eprints@whiterose.ac.uk including the URL of the record and the reason for the withdrawal request.



eprints@whiterose.ac.uk
<https://eprints.whiterose.ac.uk/>

33 such as high mechanical strength at early times of curing, high resistance to acid attack,
34 and high performance when exposed to elevated temperatures, depending on the nature
35 and dose of the precursor and activator used, and the curing conditions adopted [1-3].
36 The main raw materials typically used as precursors for alkali-activation are those which
37 are also used as supplementary cementitious materials (SCMs) in Portland cement
38 blends, such as blast furnace slag from the iron making industry, fly ashes from coal
39 combustion, and thermally treated clays such as metakaolin [4, 5]. The nature of these
40 raw materials is highly variable from source to source, and therefore, the production of
41 alkali-activated binders requires higher quality control than conventional Portland
42 cements, in order to develop specific desired properties.

43

44 Alkali-activated slag binders can develop high mechanical strengths at early times of
45 curing, with a lower permeability than identified in Portland cements [6]; however, blast
46 furnace slags are already extensively exploited by the construction industry for the
47 production of blended Portland cements. Consequently, in some parts of the world
48 different precursors are needed for the production of alkali-activated binders. As a
49 potential solution, the development of alkali-activated binders using blends of two or
50 more precursors has been carried out over the past decades, including blended systems
51 of fly ash/slag [7-10], fly ash/metakaolin [11] and slag/metakaolin [12-16]. These
52 binders usually present improved properties compared to systems where the
53 aluminosilicate precursors are activated alone, with a microstructure including co-
54 existing Ca-rich and Na-rich reaction products, depending on the fraction of the Ca-rich
55 precursor incorporated in the blend.

56

57 There is not yet a standardised methodology for dosing the alkali activator when
58 producing alkali-activated binders. This is a critical factor controlling the properties of
59 these materials, and in the case of blended activated systems it is essential to consider
60 the differences in chemistry of slag and aluminosilicate precursors, and to control the
61 kinetics of dissolution and promote the reaction of each component of the blended
62 activated binder. Typically, when a new precursor or blend is going to be activated,
63 preliminary studies are carried out to identify the amount of activator that allows the
64 production of a workable binder, with moderate initial setting time, that develops
65 compressive strengths within a desirable range, as specified by the needs of the

66 application of the final product. This means that the activator dose varies from study to
67 study, and therefore there is not a good understanding of the role of the concentration of
68 activation in the microstructural development or durability of alkali-activated materials.

69

70 Carbonation of cementitious materials is understood as the chemical reaction taking
71 place between the hydration products composing the binders and the CO₂ from the
72 atmosphere, leading to the formation of carbonates. This has been identified as one of the
73 potential disadvantages of alkali-activated binders, compared with Portland cement, as
74 the earlier studies assessing the susceptibility of degradation of these cements, via
75 acceleration carbonation tests, showed higher potential to develop carbonation problems
76 than conventional Portland cement [17-19]. Recent studies have demonstrated that the
77 mechanism of carbonation in alkali-activated binders is strongly dependent on the type
78 of the precursor used (aluminosilicates or granulated blast furnace slag) [9, 20, 21], the
79 nature of the activator [17] and the accelerated carbonation testing conditions such as
80 relative humidity [22], and CO₂ concentration [23]. Therefore, the general statement that
81 alkali-activated materials will carbonate more than Portland cement is inaccurate, as
82 there are too many variables controlling how and when carbonation of these binders is
83 going to occur, and limited correlation has been identified between natural and
84 accelerated carbonation results for alkali-activated slag materials [23].

85

86 In order to gain a better understanding of the effect of the alkali concentration on the
87 fresh paste properties of alkali-activated slag/metakaolin blends, Vicat testing and
88 isothermal calorimetry were carried out in this study. Compressive strength evolution of
89 the pastes was also tested. Mortars were produced with selected paste formulations, and
90 their resistance to accelerated carbonation was evaluated after 28 days of curing.

91

92 **2. Experimental programme**

93

94 **2.1. Materials**

95 The primary raw material used in this study was a granulated blast furnace slag (GBFS;
96 Table 1) with a basicity coefficient ($K_b = \text{CaO} + \text{MgO} / \text{SiO}_2 + \text{Al}_2\text{O}_3$) and quality coefficient
97 ($\text{CaO} + \text{MgO} + \text{Al}_2\text{O}_3 / \text{SiO}_2 + \text{TiO}_2$) of 1.01 and 1.92, respectively. Its specific gravity was 2900

98 kg/m³ and Blaine fineness 399 m²/kg. The particle size range, determined through laser
 99 granulometry, was 0.1 – 74 μm, with a d₅₀ of 15 μm.

100

101 **Table 1.** Composition of the GBFS and MK used, from X-ray fluorescence analysis. LOI is
 102 loss on ignition at 1000°C.

<i>Precursor</i>	<i>Component (mass % as oxide)</i>						<i>LOI</i>
	<i>SiO₂</i>	<i>Al₂O₃</i>	<i>CaO</i>	<i>Fe₂O₃</i>	<i>MgO</i>	<i>Other</i>	
GBFS	32.3	16.3	42.5	2.4	2.9	1.7	1.9
MK	50.7	44.6	2.7	-	-	1.0	1.0

103

104 The metakaolin (MK) used was generated in the laboratory by calcination of a kaolin
 105 containing minor quartz and dickite impurities. Calcination was carried out at 700°C in
 106 an air atmosphere, for 2 hours. The particle size range of the metakaolin was 1.8 – 100
 107 μm, with a d₅₀ of 13.2 μm and d₁₀ of 4 μm, and Blaine fineness 391 m²/kg. Alkaline
 108 activating solutions were formulated by blending a commercial sodium silicate solution
 109 with 32.4 wt.% SiO₂, 13.5 wt.% Na₂O and 54.1 wt.% H₂O, together with 50 wt.% NaOH
 110 solution, to reach overall desired molar ratios (SiO₂/Al₂O₃ (S/A) and Na₂O/Al₂O₃).

111

112 **2.2. Sample synthesis and test procedures**

113

114 **2.2.1. Pastes**

115 Pastes formulated with an overall (solid fraction in the activator + solid precursor)
 116 SiO₂/Al₂O₃ (S/A) molar ratios of 3.6, 4.0 and 4.4, GBFS/(GBFS+MK) ratios of 0.8 (20 wt.%
 117 MK), 0.9 (10 wt.% MK) and 1.0 (0 wt.% MK), with a constant water/(GBFS + MK + solid
 118 fraction in the activator) ratio of 0.23, were produced in accordance with the standard
 119 procedure ASTM C305-06 [24]. The water/solid ratio of these pastes was determined
 120 accordingly to the procedure ASTM C187 [25]. The relationship between the overall oxide
 121 ratios and the concentration of the activator (expressed as Na₂O wt.% relative to the
 122 amount of precursor to activate), is presented in Table 2. The modulus of solution (Ms =
 123 molar ratio SiO₂/Na₂O) of the activators used is between 0.9 – 1.5.

124

125 These activation concentrations are considered high for the sole activation of slag, taking
 126 into account that the conventional concentrations of activation of slag with sodium

127 silicate solution are usually between 3 – 7% Na₂O [26]; however, production of concretes
 128 with these formulations has been achieved [27, 28], which motivates the detailed
 129 understanding of the structure developed in these materials.

130

131 In fresh pastes, setting time was determined using the Vicat apparatus by following the
 132 standard procedure ASTM C191-08 [29]. The setting process of these mixes was also
 133 assessed by isothermal calorimetry (JAF calorimeter) at 25°C, over the first 40 hours of
 134 reaction. Fresh paste was mixed externally (~40g of total mix), weighed into polystyrene
 135 vessels, and immediately placed in the calorimeter.

136

137 **Table 2.** Equivalence between overall oxide ratios (precursor+activator) and activation
 138 concentration (% Na₂O by mass of GBFS + MK) used for the preparation of the pastes

139

assessed

<i>GBFS/ (GBFS+MK)</i>	<i>Overall SiO₂/Al₂O₃ ratio</i>	<i>Activation concentration (wt.%Na₂O)</i>
	4.4	10.6
1.0	4.0	9.9
	3.6	9.1
	4.4	12.5
0.9	4.0	11.6
	3.6	10.5
	4.4	14.5
0.8	4.0	13.0
	3.6	12.0

140

141 For compressive strength testing, five specimens were cast in a cylindrical mould (40 mm
 142 height and 20 mm diameter) and stored in hermetic containers at a relative humidity of
 143 90% and a temperature of 27 ± 2 °C for 1, 7, 28, 56 and 180 days.

144

145 **2.2.2. Mortars**

146 Mortars were produced with similar formulations to the pastes (Table 2), following the
 147 standard procedure ASTM C305-06 [24]. River sand with a specific gravity, absorption

148 and fineness modulus of 2450 kg/m³, 3.75% and 2.57 was used as fine aggregate. All
149 samples were formulated with a constant water/(slag + metakaolin + solid fraction in the
150 activator) ratio of 0.47 and a binder/sand ratio of 1:2.75. This water/solids ratio is
151 significantly higher than the used for producing pastes, however, it was selected in order
152 to replicate the content of water used for producing concretes with similar binder
153 formulations [27]. The specimens were cast in cubic moulds with dimensions of 50.8 x
154 50.8 mm, and stored under controlled humidity (relative humidity (RH) ~85%) and
155 ambient temperature (~25°C) for 24 h. Samples were then demoulded and cured under
156 RH of 90% and a temperature of 27 ± 2 °C for 28 days.

157

158 **2.3. Accelerated Carbonation**

159 After 28 days of curing the mortar specimens were removed from the humidity chamber,
160 dried at 60°C for 24 h, and then the top ends of the specimens were covered using an
161 acrylic resin (Acronal ®), applying a minimum of 4 layers, to direct the ingress of CO₂
162 through the selected faces of the cubes during testing. Samples were then transferred to
163 the carbonation chamber for CO₂ exposure, without application of an intermediate drying
164 or conditioning step. This was done to minimise the potential microcracking and
165 differences in sample maturity, which would be observed if they were conditioned for
166 extended periods at the testing relative humidity [22], a step which is specified in many
167 testing protocols. The conditions used were a CO₂ concentration of 1.0 ± 0.2%, a
168 temperature of 20 ± 2°C, and RH = 65 ± 5 %.

169

170 Specimens were removed from the chamber after 340 or 540 h of exposure, and the depth
171 of carbonation was measured by treating the surface of a freshly cleaved specimen with
172 a 1% solution of phenolphthalein in alcohol. In the uncarbonated part of the specimen,
173 where the mortar was still highly alkaline, purple-red colouration was obtained, while no
174 there was no colour change observed in the carbonated region. Each result is reported as
175 the average depth of carbonation measured at eight points, using two replicate samples
176 (four points per sample; the standard deviation of each carbonation depth measurement
177 is similar to or smaller than the size of the points on the graphs where plotted).

178

179 Compressive strength of carbonated and uncarbonated mortars was tested following the
180 standard procedure ASTM C 109. Capillary sorptivity, applying the standard procedure

181 SIA 162/1 [30], was also determined after the different times of CO₂ exposure (240h and
182 540h). The properties of uncarbonated samples after 28 days of curing are used as
183 reference values, indicated as zero hours of exposure.

184

185

186 **3. Results and discussion**

187

188 **3.1. Characterisation of pastes**

189 **3.1.1. Setting time**

190 All the pastes (Table 3) show shorter setting times compared with the expected for
191 conventional Portland cements [31]. Binders solely based on slag (GBFS/(GBFS+MK) =
192 1.0) formulated with increased S/A ratios (linked to higher concentrations of activation),
193 exhibit substantial increments in the initial setting time (up to 18 min), when compared
194 with pastes formulated with reduced concentrations of activation; however, the total
195 setting time reported for the samples activated with a concentration of activation ~11
196 wt.% Na₂O (S/A = 4.4) is lower than obtained when activating at reduced concentrations
197 of activator.

198

199 This behaviour differs from that which is observed in alkali-activated slag binders
200 activated under conventional activation conditions, where increased concentrations of
201 activators up to 5 wt.%Na₂O promoted reduced initial setting time. This is likely
202 associated with an increased dissolution–precipitation rate of the Ca-rich components of
203 the slag under moderate activation conditions [15, 32-34]. This indicates that the high
204 activator doses used in this study are likely hindering the solubility of Ca from the
205 dissolved slag, as it has been also identified in other studies [35, 36] where the delayed
206 Ca²⁺ precipitating in the system is prone to react with the excessive OH⁻ in the pore
207 solution forming Ca(OH)₂ instead of C-S-H type phases at early stages of reaction.

208

209

210

211

212

213 **Table 3.** Setting time of alkali silicate-activated GBFS/MK blends formulated as a
 214 function of overall molar ratios

<i>GBFS/(GBFS+MK) ratio</i>	<i>S/A ratio</i>	<i>Initial setting time (min)</i>	<i>Final setting time (min)</i>	<i>Final - Initial setting time (min)</i>
1.0	4.4	23	35	11
	4.0	11	30	19
	3.6	5	21	16
0.9	4.4	27	54	27
	4.0	46	70	24
	3.6	17	30	12
0.8	4.4	38	63	25
	4.0	34	66	32
	3.6	14	27	12

215
 216 A substantial increment in the difference between initial and final setting times is
 217 observed in pastes formulated with a GBFS/(GBFS+MK) ratio of 0.9 (10 wt.% MK) (Table
 218 3). Specifically, samples with an S/A ratio of 4.0 (~11 wt.%Na₂O) exhibited an initial
 219 setting time twice that of pastes formulated under the same conditions solely based on
 220 slag. This high concentration of activation is expected to favour the dissolution of
 221 metakaolin over the slag, which extends the setting time of the blended binders. In the
 222 activation process of metakaolin it has been identified [37] that an increased alkalinity
 223 leads to increased setting times as a consequence of the favoured dissolution of Al and Si
 224 species.

225
 226 In the blended systems, a higher content of metakaolin leads to longer setting times,
 227 which is consistent with delayed dissolution of the Ca species from the slag in the early
 228 stages of reaction. The fact that comparable total setting times are identified under the
 229 different activation conditions assessed indicate that once the dissolution and
 230 polycondensation of the Al and Si species from the metakaolin take place, the Si and Al
 231 present in the pore solution shift the speciation equilibrium and drive the dissolution of
 232 Ca by complexing with it, forming calcium silicate hydrate type gels and forcing more Ca

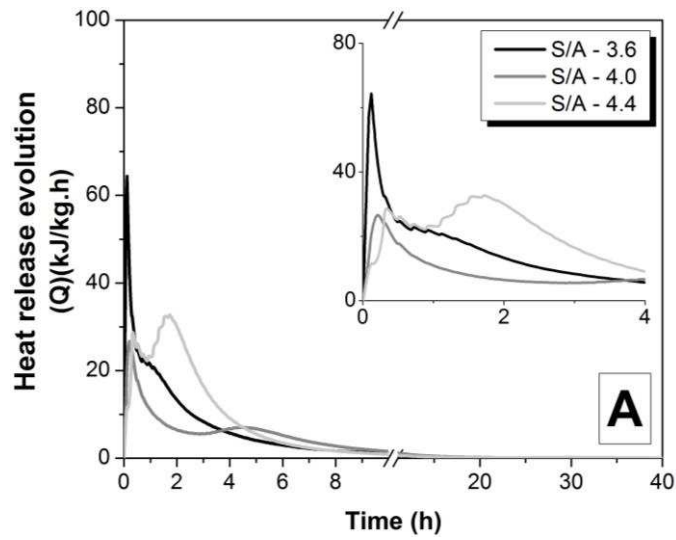
233 to dissolve. A similar effect is identified in pastes with a GBFS/(GBFS+MK) ratio of 0.8 (20
234 wt.% MK), exhibiting increased setting times when activated at higher concentrations of
235 activation.

236

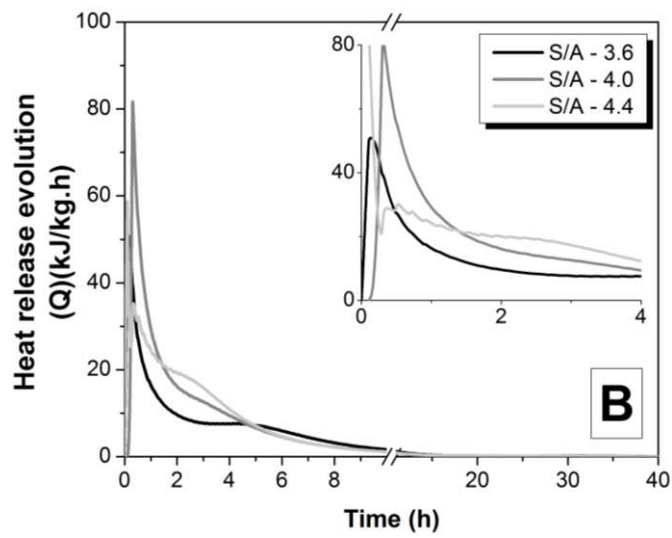
237 **3.1.2. Isothermal calorimetry**

238 Alkali activation of slag at highly alkaline concentrations induces changes in the evolution
239 of heat release (Figure 1), compared with the heat release curves reported for
240 comparable binders activated under more moderate alkaline conditions [15], which is
241 associated with modifications in the mechanism of reaction. The heat evolution curves of
242 slag-based pastes activated with an S/A ratio of 3.6 (~9 wt.% Na₂O, Figure 1A) present a
243 sharp and high intensity initial peak at the early stage of reaction, which is assigned to
244 the dissolution of slag particles and simultaneous formation of initially dissolved silicate
245 and aluminate units, as dissolution of calcium species is likely hindered under such
246 alkaline conditions.

247



248



249

250

251

252

Figure 1. Heat release of alkali-activated GBFS/MK blends with GBFS/(GBFS + MK) ratios of (A) 1.0 (0 wt.%MK), (B) 0.9 (10 wt.% MK) and (C) 0.8 (20 wt.% MK)

253 After 1 h of reaction, a second peak presenting lower intensity over an extended period
254 of time (~4 h) is observed, and attributed to the formation and subsequent precipitation
255 of the reaction products. This is consistent with the reduced initial setting times identified
256 in the pastes activated under these activation conditions, which suggests that at early
257 stages of the reaction the activation of slag under extremely high alkaline conditions
258 promotes the fast dissolution of Si-rich species, and their condensation over the surface
259 of the partially dissolved slag particles leads to the hardening of the paste. Consequently,
260 it can be suggested that the very short setting times obtained from the Vicat test may
261 correspond to early stiffening and an increased yield stress rather than true setting, and
262 thus cannot be associated with the formation of complex reaction products in the binder,
263 which takes place later in the reaction process.

264

265 At the early stage of the reaction, the slag-based paste formulated with increased
266 concentration of activation (9.9 wt.% Na₂O) presents a low intensity initial peak, which
267 is assigned to the pre-induction period of the reaction when the start of dissolution of the
268 slag particles is taking place. With the progress of the reaction, this peak shows a gradual
269 decrease in its intensity until reaching a constant value, consistent with the partial
270 initiation of an induction period. A second peak is observed after four hours of testing,
271 consistent with the acceleration–deceleration period where the precipitation of a large
272 amount of reaction products occurs.

273

274 Binders with a GBFS/(GBFS+MK) ratio of 0.9 (Figure 1B) present a single peak of heat
275 release associated with the acceleration period. An increased intensity of this peak is
276 identified at higher concentrations of activation. When samples are activated at ~11
277 wt.%Na₂O (S/A = 4.0), an increment in the total maximum heat release is identified after
278 28h of testing compared with mixes activated with lower concentrations of activation,
279 which indicates the delayed precipitation of reaction products at early age. This is
280 associated with the hindrance of the activation reaction by the excessive concentration
281 of alkalis. After the concentration of ionic species in the systems is stabilised, the reaction
282 continues to progress.

283

284 An increased concentration of activation associated with an S/A ratio of 4.4 (12.5 wt.%
285 Na₂O) promotes similar behaviour to the binders solely based on slag with S/A = 3.6,

286 consistent with the precipitation of reaction products during the first minutes of reaction,
287 followed by a sudden reduction of the heat release. For this paste two distinctive peaks
288 are observed, one between 0-1.5 h and the second between 1.5- 6 h, which suggests that
289 the precipitation of different reaction type of products is occurring as the reaction
290 proceed, consistent with the fact that an increased concentration of activation can affect
291 the dissolution of the slag in these blended systems. The greater degree of dissolution of
292 the precursors which is achieved thus enables the progressive precipitation of a higher
293 amount of reaction products than what can be expected in these systems when activated
294 under lower alkaline conditions. Significant differences in the reaction heat are not
295 identified between pastes formulated with S/A 4.0 and S/A 4.4 (Figure 1B), consistent
296 with the fact that both pastes presented similar setting times (Table 3). Those
297 formulation conditions promote the release of higher amounts of heat, when compared
298 with pastes produced at lower concentrations of activation (S/A = 3.6), associated with
299 the formation of an increased amount of reaction products.

300

301 The curves of heat release of pastes formulated with increased contents of MK in the
302 binder (20 wt.% MK, Figure 1C) present a sole asymmetric peak, attributed to the
303 acceleration period of the reaction, whose higher intensity is identified in binders
304 formulated with S/A = 3.6. This specific paste exhibit a delayed precipitation of reaction
305 products, which was not identified in binders formulated with higher concentrations of
306 activation.

307

308 With increased contents of MK ($\text{GBFS}/(\text{GBFS}+\text{MK}) = 0.8$), higher reaction heats are
309 released, indicating that increased alkalinity is favouring the enhanced dissolution of MK
310 and the consequent formation of a larger amount of reaction products. This elucidates
311 that although the MK contents in the blended systems assessed are relatively low, the
312 kinetics of reaction are strongly affected by the inclusion of this material, especially at
313 increased concentrations of activation, as consequence of the favoured dissolution and
314 polycondensation of metakaolin under these conditions [38, 39].

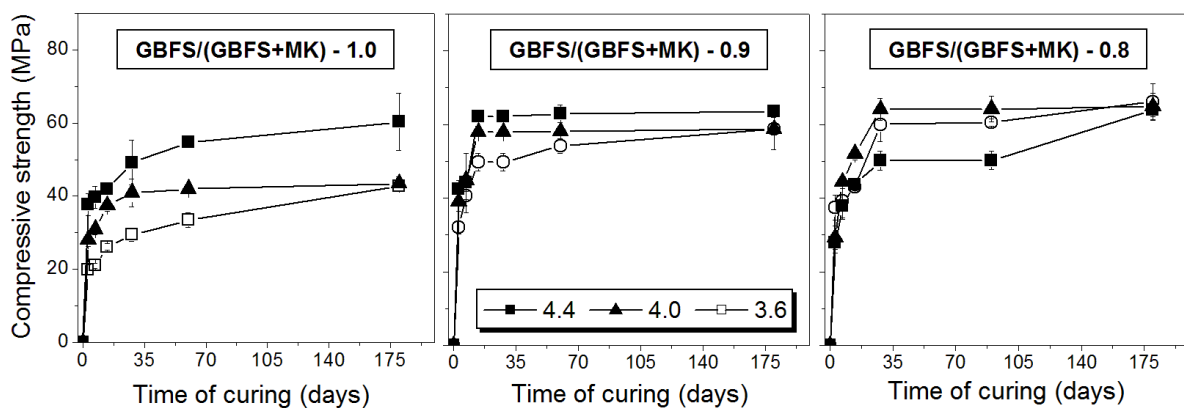
315

316 **3.1.3. Compressive strength development**

317 The compressive strengths of alkali-activated slag/metakaolin pastes cured for 180 days
318 are shown in Figure 2. Pastes based solely on slag ($\text{GBFS}/(\text{GBFS}+\text{MK}) = 1.0$) show reduced

319 compressive strength at early times of curing when formulated with an S/A ratio of 3.6;
 320 however, after 180 days of curing, similar compressive strengths to those obtained in
 321 activated slag pastes formulated with higher S/A are achieved. Higher S/A ratios (4.4)
 322 promote the development of higher mechanical strength, especially at longer times of curing
 323 curing. Specimens with a GBFS/(GBFS+MK) ratio of 0.9 (Figure 2) have slightly higher
 324 mechanical strength at early times of curing than the slag-only pastes at all of the S/A
 325 ratios assessed. This indicates that the metakaolin included in the binder is effectively
 326 reacting, as observed in the calorimetry results (Figure 1), and it is contributing to the
 327 enhancement of the mechanical strength of the blended binder. The microstructural
 328 characterisation of pastes with similar formulations to the used in this study showed [40]
 329 that formation of strength giving phases such as C-(N)-A-S-H along with the zeolites
 330 gismondine and garronite is taking place in these systems since early times of reaction,
 331 despite the high concentration of activation used, and its potential effect in the
 332 dissolution of Ca from the slag. These reaction products slightly differ from those
 333 typically identified in alkali-activated slag systems produced with lower contents of
 334 activator [1], but they are clearly contributing to the strength development of these
 335 binders.

336
 337



338
 339 **Figure 2.** Compressive strength of alkali-activated GBFS/MK blends with
 340 GBFS/(GBFS + MK) ratios as shown in each image, as a function of the activation
 341 conditions (S/A ratios listed in legend)
 342

343 For pastes formulated with S/A = 3.6 the mechanical development seems to be slightly
 344 delayed compared with the specimens with higher S/A ratios, as the compressive

345 strength exhibited by these samples is slightly lower until 90 days of curing, and
346 comparable to the other pastes after 180 days of curing when metakaolin is included in
347 the formulations. Under high alkalinity conditions and with metakaolin present, values
348 close to the ultimate strengths are obtained after just 28 days of curing, indicating that
349 these activating conditions accelerate the structural development at early times of curing.

350

351 Reduced S/A ratios, associated with increased concentrations of activation, favour the
352 development of higher mechanical strengths in pastes with a GBFS/(GBFS+MK) ratio of
353 0.8. Those specimens exhibited substantial increments in the mechanical strength during
354 the first days of curing, being higher in the case of pastes activated with S/A ratio of 3.6
355 and 4.0. The mechanical development seems to be delayed when specimens are produced
356 with increased S/A ratio (4.4); however, comparable compressive strength values are
357 obtained for these mixes at the three activation conditions assessed after 180 days of
358 curing.

359

360 These results are consistent with the kinetics of reaction identified through the
361 calorimetry study (Figure 1), indicating that increased concentrations of activation,
362 associated with higher S/A ratio, favour the dissolution and precipitation of a higher
363 amount of reaction products in specimens including MK as these conditions favour the
364 dissolution and consequent polycondensation of binding gels. The mechanical strengths
365 obtained for pastes solely based on slag are lower than those presented in previous
366 reports assessing the same slag under less-alkaline activation conditions [15]. Those
367 obtained for pastes with GBFS/(GBFS+MK) ratios of 0.9 and 0.8 are somehow consistent
368 with the hindering of the Ca^{2+} dissolution from the slag under the activation conditions
369 used, potentially delaying the formation of binding phases, and consequently promoting
370 reduced mechanical strengths at early times of curing. These results suggest that even
371 though the reaction of the slag is hindered using the activation conditions adopted in
372 study, the effective activation of the metakaolin included is achieved, and the later
373 strengths (70 – 80 MPa) at 180 days of curing are characteristic of high performance
374 materials.

375

376

377

378 3.2. Accelerated carbonation performance of mortars

379

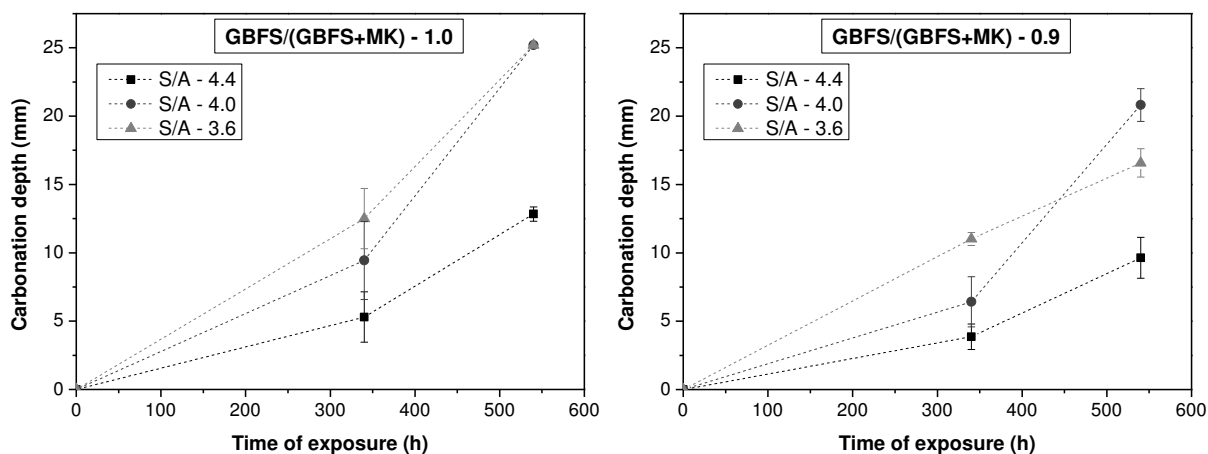
380 3.2.1. Carbonation depth

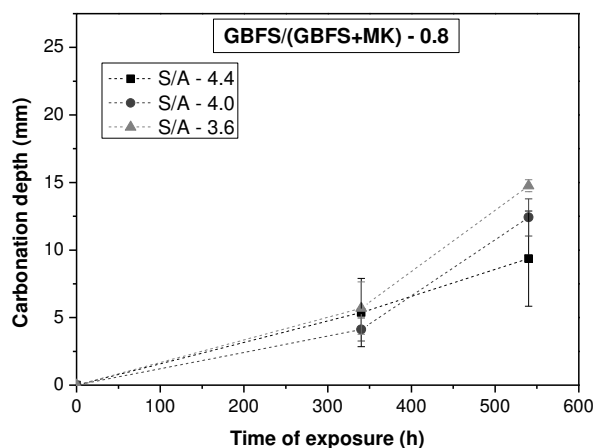
381 In Figure 3A it can be seen that there is a reduction in the carbonation depth in mortars
382 of alkali-activated slag, as the concentration of activation increases. Specimens
383 formulated with an S/A ratio of 4.4 exhibited a carbonation depth of 21%, after 340h of
384 exposure to 1% CO₂, while samples formulated with S/A ratios of 4.0 and 3.6 present
385 carbonation depths of 42% and 37% respectively. After 540h of CO₂ exposure, the
386 mortars produced with S/A ratio of 4.4 exhibited a carbonation depth of 51%, conversely
387 the mortars formulated with reduced concentrations of activation, where the 50.8 mm
388 mortar cube samples were fully carbonated after 540h of CO₂ exposure.

389

390 In mortars produced with a GBFS/(GBFS+MK) of 0.9 (Figure 3B) a similar trend is
391 identified, so that a higher concentration of activation promotes reduced carbonation
392 depths in the mortars. After 340h of CO₂ exposure the blended slag/metakaolin mortars
393 formulated with S/A = 3.6 exhibited a carbonation depth 8% higher than was observed
394 in activated slag-only mortars produced with a similar concentration of activation (S/A =
395 4.4). In these blended binders formulated with S/A = 4.4, carbonation depth reductions
396 of up to 65% are identified when compared with the carbonation values identified in
397 samples formulated with lower S/A ratios. After 540h of CO₂ exposure, unlike the slag-
398 only binders, these samples did not reach full carbonation.

399





400 **Figure 3.** Carbonation depth of mortars based on activated slag/metakaolin blended
 401 binders as a function of the GBFS/(GBFS+MK) ratio and activation concentration

402
 403 In mortars formulated with a GBFS/ (GBFS+MK) ratio of 0.8 no significant differences in
 404 the carbonation depth are identified for the different activation conditions adopted in this
 405 study, especially after 340h of CO₂ exposure. However, after 540h of CO₂ exposure it is
 406 possible to identify (Figure 3C) that higher concentrations of activation (associated with
 407 higher S/A ratios) lead to a reduced progress of carbonation. It is worth noting that
 408 carbonation depths of these activated blended mortars are significantly lower than those
 409 identified in mortars with lower contents of metakaolin, independent of the
 410 concentration of activation used.

411
 412 It is important to note that these results differ from the identified by Burciaga-Diaz et al.
 413 [41] who reported that increased concentrations of activation and addition of metakaolin
 414 in alkali activated slag binders led to severe carbonation damage of the specimens. In
 415 order to elucidate why different results have been identified, it is important to consider
 416 the differences in the chemistry of the slag used by Burciaga-Diaz [41] and the slag used
 417 in this study (Table 1). The slag used in that study is richer in MgO (8.9 wt%) and has
 418 reduced CaO (37.8 wt.%), compared to that used in the present study. The role of the
 419 composition of the slag in the determining carbonation resistance of alkali-activated
 420 binders has recently been elucidated [21], so that higher contents of MgO in the slag
 421 favour the formation of hydrotalcite type reaction products, which can absorb CO₂,
 422 enhancing the carbonation resistance of alkali-activated slag binders. Therefore, it might
 423 be expected that the binders produced by Burciaga-Diaz et al. [41] will perform better

424 under accelerated carbonation conditions, than those produced in this study with lower
425 MgO content.

426

427 However, the kinetics of reaction of these two slags are completely different. In slags with
428 a higher MgO content than the one used in the present study (2.87 wt.%), such as the slag
429 used by Fernández-Jiménez et al. [42], an increased concentration of activation (>5 wt.%
430 Na₂O) reduces the degree of reaction of the slag. Similar results have been identified by
431 the author (unpublished data) where a threshold value of concentration of activation is
432 typically identified, and increased concentrations of activation reduce the slag reactivity
433 as the MgO content in the slag increases. Conversely, in the low MgO content slag used in
434 this study it has been identified [15] that a higher concentration of alkalis in the system
435 favours a higher degree of reaction of the slag.

436

437 Therefore, there is no single factor that can explain the carbonation results identified the
438 activated slag/metakaolin binders assessed in the present study, as there are several
439 important parameters playing a significant role in how carbonation progresses in these
440 systems, including:

- 441 • the evolution of the alkalinity of the pore solution upon carbonation, as the pore
442 water can act as a CO₂ sorbent in presence of high CO₂ concentrations [23],
- 443 • the chemistry and microstructure of the reaction products formed, as the nature
444 and Ca/Si ratios of the C-A-S-H forming in these systems will influence the
445 decalcification process taking place in these binders , and
- 446 • the changes in permeability of these materials during accelerated carbonation, at
447 the different concentrations of activation and contents of metakaolin added to the
448 system, as this controls the diffusivity of CO₂ within the samples. This will be
449 addressed in detail below, as sorptivity data for the mortars assessed will be
450 reported in Section 3.2.3.

451 Consequently, detailed microstructural characterisation of these binders after
452 carbonation is required to elucidate the role of the chemistry of the reaction products
453 forming in the carbonation reaction.

454

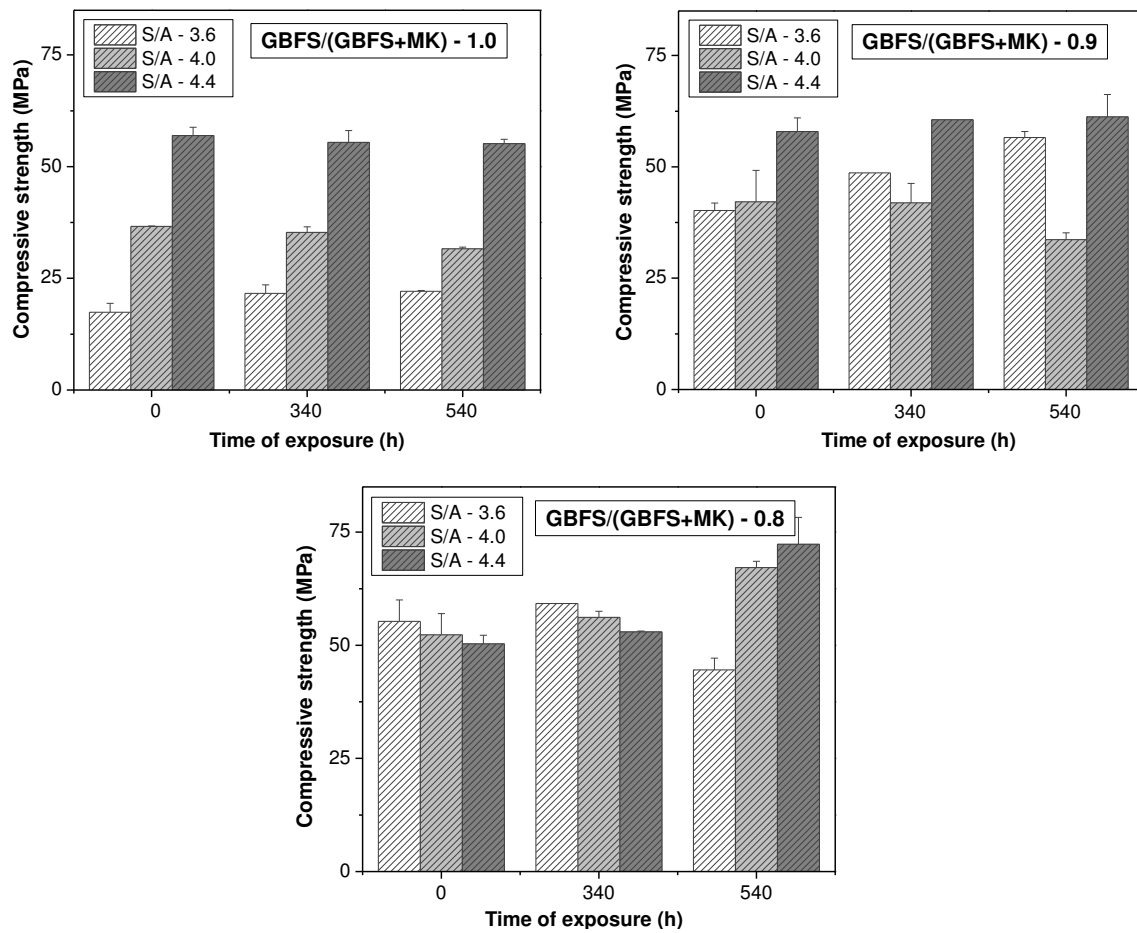
455 **3.2.2. Residual compressive strength**

456 Mortars based solely on activated slag (Figure 4A) developed comparable compressive
457 strength than the corresponding paste specimens (Figure 2) at 28 days of curing, with no
458 significant changes when using different concentrations of activation. Upon carbonation
459 for 340 h, the specimens retained their original compressive strength, despite the
460 observation (Figure 3) that significant carbonation is taking place in these specimens. A
461 longer time of CO₂ exposure does not generally seem to impact the compressive strength
462 of the samples, although a slight reduction (14%) is solely observed in the mortar
463 formulated with S/A = 4.0.

464

465 In carbonated plain Portland cement systems, increments in the compressive strength
466 with carbonation are typically identified [43, 44], which has been associated with the
467 precipitation of a large amount of calcium carbonate as carbonation products, which
468 provides more contribution to strength than the portlandite it replaces. Conversely, in
469 alkali-activated slag materials, carbonation typically leads to a substantial decrease in the
470 compressive strength [45], associated with the decalcification of the main binding phase,
471 C-A-S-H type gel, along with an increase in permeability. Considering that in alkali-
472 activated slags produced at high [40] and moderate alkalinity [15], formation of
473 comparable reaction products has been identified, it is therefore likely suggest that the
474 hyperalkaline pore solution generated in the binders produced in this study is instead
475 determining the kinetics and impacts of carbonation. In particular, it seems that in this
476 instance carbonation of the pore solution and precipitation of carbonation products
477 contributes to the blockage of the pores, reducing the permeability of the system.

478



479 **Figure 4.** Residual compressive strength of carbonated mortars based on
 480 slag/metakaolin activated blends as function of the time of exposure to 1% CO₂
 481

482 Under the activation conditions used here, a significant increase in the compressive
 483 strength is identified with the inclusion of higher contents of metakaolin, consistent with
 484 a larger extent of reaction of the metakaolin as the concentration of activation increases,
 485 as identified by isothermal calorimetry (Figure 1). Mortars formulated with a
 486 GBFS/(GBFS+MK) ratio of 0.9 exposed to CO₂ for 340 h exhibited an increase in the
 487 compressive strength by up to 35% when the samples were formulated with S/A = 3.6,
 488 which is entirely contrary to previous reports [45] of strength losses in alkali-activated
 489 binders upon carbonation. No significant differences in strength as a function of
 490 carbonation duration were identified in the carbonated specimens formulated with S/A
 491 ratios of 4.0 and 4.4. This might be a combined effect of the initial carbonation of the pore
 492 solution followed by the gradual progress of carbonation of the reaction products of these
 493 samples (less than 10 mm between 340h and 540h of CO₂ exposure), and the progressive
 494 activation reaction taking place in the uncarbonated cores of the specimens generating

495 additional strength. The addition of 20 wt.% MK in these binders does not induce any
496 significant changes in the strength of the mortars upon CO₂ exposure for 340 h. However,
497 after 540 h of CO₂ exposure, the mortars formulated with a S/A ratio of 3.6 exhibited a
498 compressive strength loss of up to 27%. Conversely, in mortars formulated with lower
499 S/A ratios, significant increases in the compressive strength are identified.

500

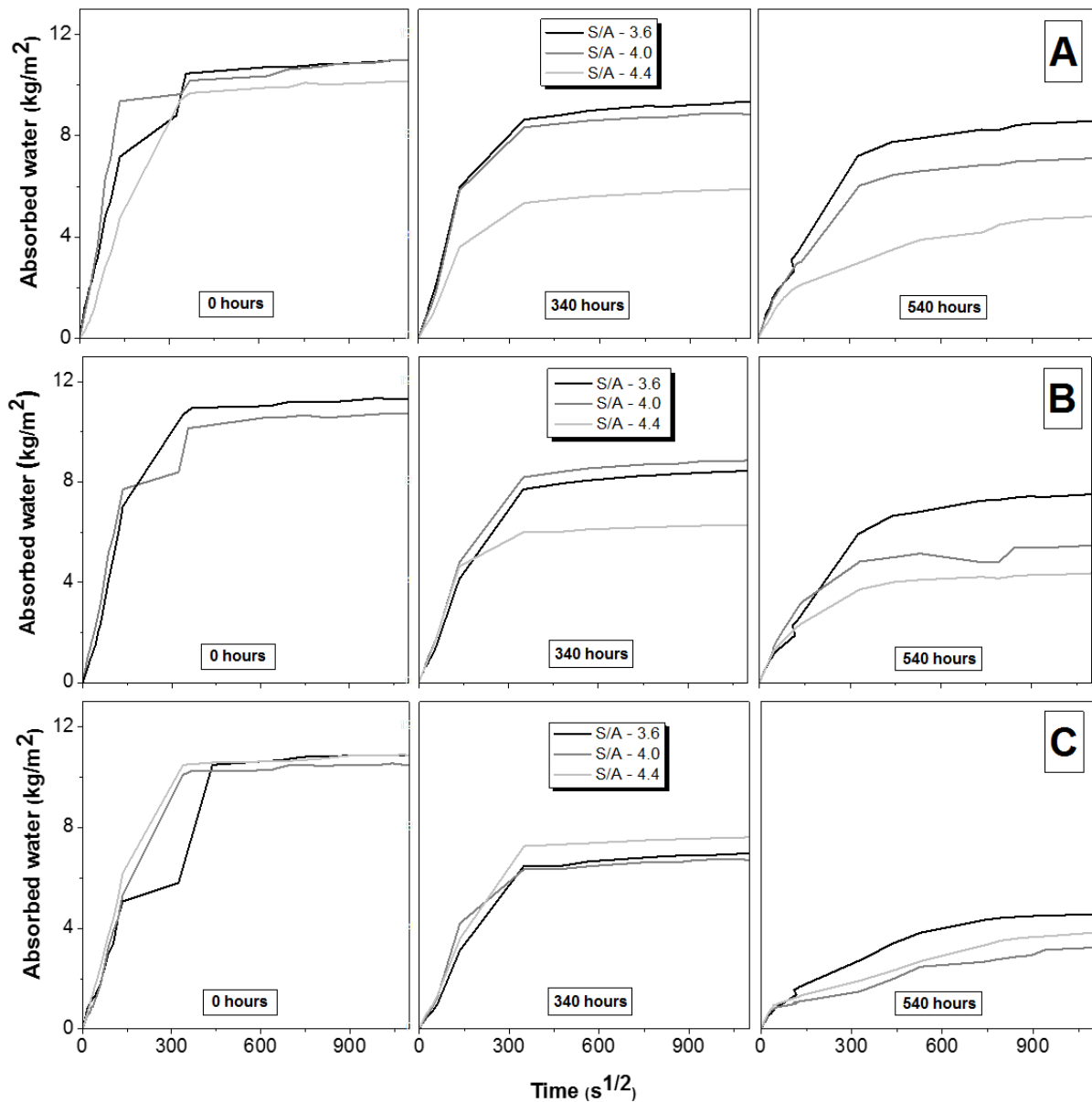
501 There does not seem to be a correlation between the carbonation depth identified for
502 these mortars and the compressive strength determined at the different times of
503 exposure, especially in the case of alkali-activated slag mortars, where the samples were
504 fully carbonated after 540h of CO₂ exposure, but still retained compressive strengths of
505 up to 50 MPa. It has been discussed [45] that the phenolphthalein method is not a reliable
506 test for measuring the carbonation of alkali-activated materials, as this is a measurement
507 of the alkalinity of the system, and it does not give any information regarding any
508 structural changes taking place in these binders upon CO₂ exposure. The reaction
509 products forming in alkali-activated materials are not themselves alkaline, as it is the case
510 of portlandite in hydrated Portland cement, and all of the alkalinity is held in the pore
511 solution. Therefore, the phenolphthalein measurement, reported in this study as
512 carbonation depth, might be solely showing the regions where carbonation of the pore
513 solution has taken place, rather than potential decay of the main binding phases.

514

515 **3.2.3. Capillary sorptivity**

516 Sorptivity curves of the mortars assessed are shown in Figure 5. In all specimens reduced
517 water absorption is observed in the partially carbonated samples, particularly at
518 extended times of CO₂ exposure. This indicates that the retention of compressive strength
519 of the activated slag/metakaolin mortars can be at least partially explained by refinement
520 of the pore structure, due to precipitation of large amounts of carbonation products. This
521 observation differs from what has been obtained in carbonated specimens with similar
522 contents of metakaolin but activated with reduced activator concentrations [20], in
523 alkali-activated slag specimens [19, 46] and even in concrete specimens with similar
524 binder formulations [22], where accelerated carbonation induced an increase in capillary
525 permeability and water absorption of the material. It is likely that the large fraction of
526 paste in the mortars, compared with the concretes produced with a similar binder

527 formulation in [22], favours formation of a higher amount of carbonation products,
 528 hindering the ingress of CO₂ in the specimens.
 529



530
 531 **Figure 5.** Capillary sorptivity curves of uncarbonated (0 hours) and carbonated (340
 532 and 540 hours) alkali-activated slag/metakaolin mortars, as a function of the MK
 533 content: GBFS/(GBFS+MK) = (A) 1.0, (B) 0.9, (C) 0.8
 534

535 Regardless of the concentration of activation and the content of metakaolin in the binder,
 536 after 340h of CO₂ exposure, all the mortars showed (Table 4) a decrease in the capillary
 537 coefficient (k , the initial slopes of the sorptivity plots in Figure 5) of up to 40%, when
 538 compared with non-carbonated samples. Similar results are observed in specimens

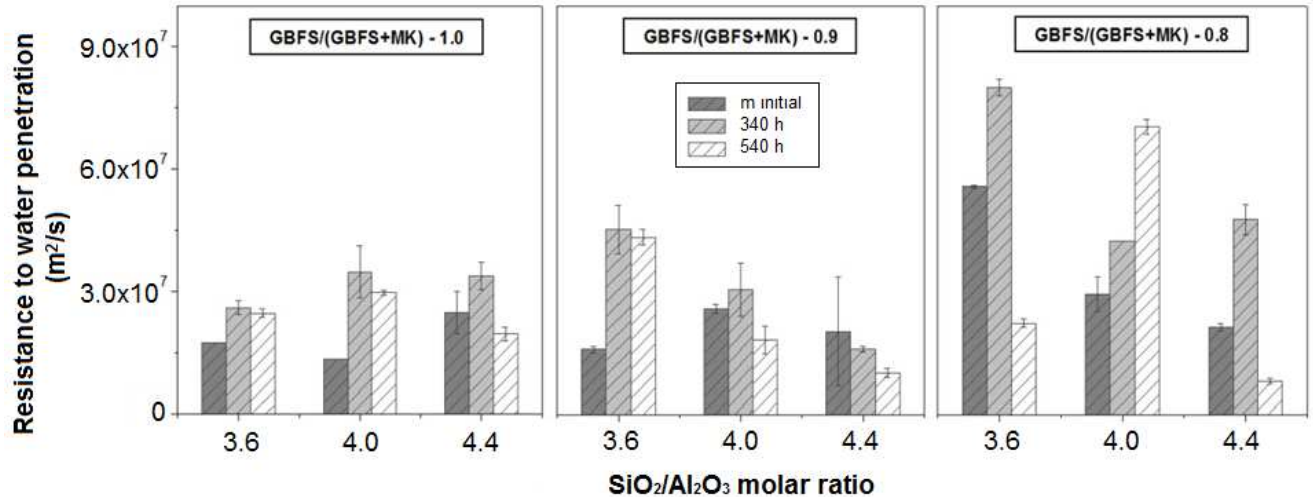
539 exposed to CO₂ for 540h. Lower *k* values are associated with a reduced capillary
 540 sorptivity, indicating a decrease in the total porosity of the specimens. In all the mortars
 541 assessed, the exposure to CO₂ induced an increment in the resistance to water
 542 penetration (*m*) (Figure 6), consistent with the reduction in the capillary coefficient (*k*).
 543 Carbonated mortars solely based on slag and activated with the lower concentration of
 544 activation (S/A – 3.6) report resistance to water penetration values three times higher
 545 than observed in non-carbonated reference samples. A similar trend was in observed in
 546 mortars including 10 wt% of MK (GBFS/(GBFS+MK) – 0.9) when activated at a similar
 547 concentration of activation. In the other specimens, the increments in the resistance of
 548 water penetration coefficient were up to 40%.

549

550 **Table 3.** Capillary sorptivity coefficients of alkali-activated slag/metakaolin mortars as
 551 function of the time of CO₂ exposure

<i>GBFS/(GBFS+MK)</i> <i>ratio</i>	<i>SiO₂/Al₂O₃</i>	<i>k (kg/m².s^{1/2})</i>		
		<i>0 h</i>	<i>340 h</i>	<i>540 h</i>
1.0	3.6	0.052	0.038	0.033
	4.0	0.061	0.031	0.026
	4.4	0.039	0.021	0.021
0.9	3.6	0.051	0.024	0.024
	4.0	0.048	0.030	0.027
	4.4	-	0.029	0.027
0.8	3.6	0.029	0.016	0.018
	4.0	0.036	0.020	0.023
	4.4	0.043	0.021	0.025

552



553

554 **Figure 6.** Resistance to water penetration of alkali-activated slag/metakaolin mortars,
 555 as function of the activation conditions and time of exposure to CO₂

556

557 4. Conclusions

558

559 The high alkalinity conditions adopted in this study to produce activated slag/metakaolin
 560 blended binders affects the kinetics of reaction of the slag used, so that a higher
 561 concentration of activation increased the initial setting times of the pastes, however the
 562 time between initial and final setting of the activated slag binders was shortened as the
 563 concentration of activation increased. The inclusion of metakaolin increases the total
 564 setting time of the pastes produced from this unusually low-MgO slag, independent of the
 565 amount incorporated and the concentration of activation used. This might be a
 566 consequence of the combined effect of reduced dissolution of Ca from the slag, along with
 567 a high dissolution of Al and Si species from metakaolin, which are favoured under the
 568 highly alkaline conditions adopted. As the alkalinity in the binders is increased at higher
 569 activator concentrations, the reaction of the system is governed by the dissolution and
 570 polycondensation of the species from the metakaolin. The alkali-activated slag binders
 571 tested here, at high activator concentrations, developed lower compressive strengths
 572 than have been achieved when activating this slag under milder concentrations. Under
 573 the activation conditions adopted here, the inclusion of metakaolin led to a significant
 574 increase in the compressive strength, associated with the simultaneous reaction of slag
 575 and metakaolin.

576

577 A reduced rate of carbonation was identified in these materials with the addition of
578 metakaolin, and also with increasing the concentration of the activator. Little or no loss
579 of compressive strength, and significant reductions in the water permeability, were
580 observed at longer times of CO₂ exposure. This suggest that under the activation
581 conditions used, precipitation of a large amount of carbonation products might be taking
582 place as a result of interactions between the highly alkaline pore solution and the
583 incoming CO₂, refining the pore network of the mortars. This hindered the ingress of CO₂
584 within the samples and therefore reduced the carbonation progress. It is important to
585 note that no correlation could be identified between the carbonation front determined
586 using a phenolphthalein indicator, and the compressive strength and water sorption of
587 the test samples. The phenolphthalein indicator is revealing the regions where reductions
588 of the pH are taking place as a consequence of the carbonation of the pore solution, rather
589 than regions where damage to the strength-giving binder products is occurring.
590 Therefore, the methods used for measurement of carbonation depth in alkali-activated
591 materials requires reassessment, as the standard approach using a phenolphthalein
592 indicator may not be providing accurate information.

593

594

595 **5. Acknowledgments**

596

597 This study was sponsored by *Universidad del Valle* (Colombia) and COLCIENCIAS. Prof.
598 Ruby Mejía de Gutierrez (U. del Valle) and Prof. John Provis (U. Sheffield) are greatly
599 acknowledged for their guidance and valuable discussions.

600

601 **6. References**

602

603 [1] Provis JL, Bernal SA. Geopolymers and related alkali-activated materials. *Annu Rev Mater Res*
604 2014;44:299-327.

605 [2] Provis JL. Green concrete or red herring? - the future of alkali-activated materials. *Adv Appl*
606 *Ceram* 2014;113(8):472-7.

607 [3] Provis JL. Geopolymers and other alkali activated materials: why, how, and what? *Mater Struct*
608 2014;47(2):11-25.

609 [4] Duxson P, Provis JL. Designing precursors for geopolymer cements. *J Am Ceram Soc*
610 2008;91(12):3864-9.

- 611 [5] Shi C, Fernández-Jiménez A, Palomo A. New cements for the 21st century: The pursuit of an
612 alternative to Portland cement. *Cem Concr Res* 2011;41(7):750-63.
- 613 [6] Bernal SA, Bílek V, Criado M, Fernández-Jiménez A, Kavalerova E, Krivenko PV, et al. Durability
614 and Testing–Degradation via Mass Transport. In: Provis JL, Van Deventer JSJ, editors. *Alkali*
615 *Activated Materials*: Springer; 2014. p. 223-76.
- 616 [7] Puertas F, Fernández-Jiménez A. Mineralogical and microstructural characterisation of alkali-
617 activated fly ash/slag pastes. *Cem Concr Compos* 2003;25(3):287-92.
- 618 [8] Ismail I, Bernal SA, Provis JL, Hamdan S, van Deventer JSJ. Microstructural changes in alkali
619 activated fly ash/slag geopolymers with sulfate exposure. *Mater Struct* 2013;46(3):361-73.
- 620 [9] Bernal SA, Provis JL, Walkley B, San Nicolas R, Gehman J, Brice DG, et al. Gel nanostructure in
621 alkali-activated binders based on slag and fly ash, and effects of accelerated carbonation. *Cem*
622 *Concr Res* 2013;53:127-44.
- 623 [10] Dombrowski K, Buchwald A, Weil M. The influence of calcium content on the structure and
624 thermal performance of fly ash based geopolymers. *J Mater Sci* 2007;42(9):3033-43.
- 625 [11] Ruiz-Santaquiteria C, Skibsted J, Fernández-Jiménez A, Palomo A. Alkaline solution/binder
626 ratio as a determining factor in the alkaline activation of aluminosilicates. *Cem Concr Res*
627 2012;42(9):1242-51.
- 628 [12] Buchwald A, Hilbig H, Kaps C. Alkali-activated metakaolin-slag blends – Performance and
629 structure in dependence on their composition. *J Mater Sci* 2007;42(9):3024-32.
- 630 [13] Yip CK, Lukey GC, Provis JL, van Deventer JSJ. Effect of calcium silicate sources on
631 geopolymerisation. *Cem Concr Res* 2008;38(4):554-64.
- 632 [14] Bernal SA, Rodríguez ED, Mejía de Gutierrez R, Gordillo M, Provis JL. Mechanical and thermal
633 characterisation of geopolymers based on silicate-activated metakaolin/slag blends. *J Mater Sci*
634 2011;46(16):5477-86.
- 635 [15] Bernal SA, Provis JL, Mejía de Gutierrez R, Rose V. Evolution of binder structure in sodium
636 silicate-activated slag-metakaolin blends. *Cem Concr Compos* 2011;33(1):46-54.
- 637 [16] Burciaga-Díaz O, Magallanes-Rivera R, Escalante-García J. Alkali-activated slag-metakaolin
638 pastes: strength, structural, and microstructural characterization. *J Sust Cem-Based Mater*
639 2013;2(2):111-27.
- 640 [17] Palacios M, Puertas F. Effect of carbonation on alkali-activated slag paste. *J Am Ceram Soc*
641 2006;89(10):3211-21.
- 642 [18] Deja J. Carbonation aspects of alkali activated slag mortars and concretes. *Silic Industr*
643 2002;67(1):37-42.
- 644 [19] Puertas F, Palacios M, Vázquez T. Carbonation process of alkali-activated slag mortars. *J*
645 *Mater Sci* 2006;41:3071-82.
- 646 [20] Bernal SA, Mejía de Gutierrez R, Rose V, Provis JL. Effect of silicate modulus and metakaolin
647 incorporation on the carbonation of alkali silicate-activated slags. *Cem Concr Res*
648 2010;40(6):898-907.

- 649 [21] Bernal SA, San Nicolas R, Myers RJ, Mejía de Gutiérrez R, Puertas F, van Deventer JSJ, et al.
650 MgO content of slag controls phase evolution and structural changes induced by accelerated
651 carbonation in alkali-activated binders. *Cem Concr Res* 2014;57:33-43.
- 652 [22] Bernal SA, Provis JL, Mejía de Gutiérrez R, van Deventer JSJ. Accelerated carbonation testing
653 of alkali-activated slag/metakaolin blended concretes: effect of exposure conditions. *Mater Struc*
654 2015;48:653-69.
- 655 [23] Bernal SA, Provis JL, Brice DG, Kilcullen A, Duxson P, van Deventer JSJ. Accelerated
656 carbonation testing of alkali-activated binders significantly underestimate the real service life:
657 The role of the pore solution. *Cem Concr Res* 2012;42(10):1317-26.
- 658 [24] ASTM international. Standard practice for mechanical mixing of hydraulic cement pastes and
659 mortars of plastic consistency (ASTM C305-06).
- 660 [25] ASTM international. Standard test method for amount of water required for normal
661 consistency of hydraulic cement paste (ASTM C187).
- 662 [26] Shi C, Krivenko PV, Roy DM. *Alkali-Activated Cements and Concretes*. Abingdon, UK: Taylor
663 & Francis; 2006.
- 664 [27] Bernal SA, Mejia de Gutierrez R, Provis JL. Engineering and durability properties of concretes
665 based on alkali-activated granulated blast furnace slag/metakaolin blends. *Constr Build Mater*
666 2012;33:99-108.
- 667 [28] Bernal SA, Mejía de Gutiérrez R, Ruiz F, Quiñones H, Provis JL. High-temperature
668 performance of mortars and concretes based on alkali-activated slag/metakaolin blends. *Mater*
669 *Construc* 2012;62(308):471-88.
- 670 [29] ASTM international. Standard test methods for time of setting of hydraulic cement by vicat
671 needle (ASTM C191-08).
- 672 [30] Fagerlund G. On the capillarity of concrete. *Nord Concr Res* 1982;1:6.1-6.20.
- 673 [31] Hewlett PC. *Lea's Chemistry of Cement and Concrete*, 4th Ed. Oxford, UK: Elsevier; 1998.
- 674 [32] Chang JJ. A study on the setting characteristics of sodium silicate-activated slag pastes. *Cem*
675 *Concr Res* 2003;33(7):1005-11.
- 676 [33] Živica V. Effects of type and dosage of alkaline activator and temperature on the properties
677 of alkali-activated slag mixtures. *Constr Build Mater* 2007;21(7):1463-9.
- 678 [34] Song S, Sohn D, Jennings HM, Mason TO. Hydration of alkali-activated ground granulated
679 blast furnace slag. *J Mater Sci* 2000;35:249-57.
- 680 [35] Yip CK, Lukey GC, van Deventer JSJ. The coexistence of geopolymeric gel and calcium silicate
681 hydrate at the early stage of alkaline activation. *Cem Concr Res* 2005;35(9):1688-97.
- 682 [36] Burciaga-Díaz O, Escalante-García JI. Structure, mechanisms of reaction, and strength of an
683 alkali-activated blast-furnace slag. *J Am Ceram Soc* 2013;96(12):3939-48.
- 684 [37] Xu H, van Deventer JSJ. The geopolymerisation of alumino-silicate minerals. *Int J Miner Proc*
685 2000;59(3):247-66.

- 686 [38] Granizo ML, Blanco MT. Alkaline activation of metakaolin - An isothermal conduction
687 calorimetry study. *J Therm Anal* 1998;52(3):957-65.
- 688 [39] Granizo ML, Blanco Varela MT, Martínez-Ramírez S. Alkali activation of metakaolins:
689 Parameters affecting mechanical, structural and microstructural properties. *J Mater Sci*
690 2007;42(9):2934-43.
- 691 [40] Bernal SA, Provis JL, Rose V, Mejía de Gutiérrez R. High-resolution X-ray diffraction and
692 fluorescence microscopy characterization of alkali-activated slag-metakaolin binders. *J Amer*
693 *Ceram Soc* 2013;96 (6):1951-7.
- 694 [41] Burciaga-Díaz O, Escalante-García JI, Arellano-Aguilar R, Gorokhovskiy A. Statistical analysis
695 of strength development as a function of various parameters on activated metakaolin/slag
696 cements. *J Am Ceram Soc* 2010;93(2):541-7.
- 697 [42] Fernández-Jiménez A, Puertas F. Influence of the activator concentration on the kinetics of
698 the alkaline activation process of a blast furnace slag. *Mater Constr* 1997;47(246):31-42.
- 699 [43] Lange LC, Hills CD, Poole AB. The effect of accelerated carbonation on the properties of
700 cement-solidified waste forms. *Waste Manage* 1996;16(8):757-63.
- 701 [44] Lange LC, Hills CD, Poole AB. Effect of carbonation on properties of blended and non-blended
702 cement solidified waste forms. *J Hazard Mater* 1997;52(2-3):193-212.
- 703 [45] Bernal SA. The resistance of alkali-activated cement-based binders to carbonation. In:
704 Pacheco-Torgal F, Labrincha J, Leonelli C, Palomo A, Chindaprasit P, editors. *Handbook of Alkali-*
705 *Activated Cements, Mortars and Concretes*. Cambridge, UK: Woodhead Publishing; 2014. p. 319-
706 29.
- 707 [46] Rodríguez E, Bernal S, Mejía de Gutierrez R, Puertas F. Alternative concrete based on alkali-
708 activated slag. *Mater Constr* 2008;58(291):53-67.
709
- 710
- 711